# Monte Carlo simulation of master equations
# in quantum optics for vacuum, thermal, and squeezed reservoirs

R. Dum, A. S. Parkins, and P. Zoller

*Joint Institute for Laboratory Astrophysics, University of Colorado, Boulder, Colorado 80309-0440*

C. W. Gardiner

*Department of Physics, University of Waikato, Hamilton, New Zealand*

Wave-function simulation of the master equation in terms of quantum jumps is illustrated for vacuum, thermal, and squeezed reservoirs. We discuss simulation techniques for (i) atomic density matrices, and resonance fluorescence and weak-field absorption spectra of atoms, (ii) decay of a two-level system in a squeezed vacuum, and (iii) a strongly coupled atom-cavity system driven by thermal light.

PACS number(s): 42.50.Lc

## I. INTRODUCTION

Damping and fluctuations in quantum mechanics can be described by coupling a system to a heat bath. Eliminating the heat bath in the Markov approximation leads to a master equation for the *reduced density operator* of the system [1]. In a series of recent papers simulation of the quantum master equation in terms of *system wave functions* has been proposed [2–6]. Apart from the interesting conceptual questions that arise in the simulation of quantum noise, the problem is of significant practical interest in seeking a solution of the master equation for systems with a large number of degrees of freedom close to the quantum limit, in particular in the context of quantum optics. Our work in this context has been based on propagating a system wave function with a non-Hermitian (damped) system Hamiltonian and simulating a sequence of *quantum jumps* [7] of the system according to a *delay function* for the occurrence of the "next jump" [2, 3]. Dalibard, Castin, and Mølmer [4] and Carmichael [5] have formulated a simulation method in which a sequence of fictitious measurements are performed at small discrete (fixed) time steps.

In Ref. [2] we have presented a simulation approach for an atomic system undergoing spontaneous emission (an atom driven by a laser and coupled to vacuum modes) including mechanical light effects. This work has been based on reinterpreting Mollow's pure state analysis of resonant light scattering [8] in terms of a simulation prescription. In Ref. [3] we have derived a general formalism for vacuum, thermal, and squeezed reservoirs from the point of view of the Srinivas-Davies theory of continuous measurements [9], and have connected this approach to an Ito calculus for a stochastic Schrödinger equation. The purpose of the present paper is to illustrate this wave-function simulation method for vacuum, thermal, and squeezed noise by specific examples in a quantum-optics context. In addition, we discuss in some detail a simulation procedure for system spectra and correlation

functions.

The paper is organized as follows. In Sec. II we give a brief summary of the simulation method. In Sec. III we present the calculation of photon statistics [1, 10], and the Mollow resonance fluorescence and absorption spectrum of a two-level system driven by a strong laser field [11, 12]. Our approach to calculating the spectra relies on introducing a coupling of the system to weak (external) probe fields. This gives rise to a set of equations for the first-order perturbed wave functions which are propagated according to a sequence of quantum jumps dictated by the particular realization of the zeroth-order system wave function (see also Ref. [8]). In Sec. IV we simulate quantum jumps for a two-level system coupled to a squeezed vacuum which leads to inhibition of phase decay [13]. Finally, in Sec. V we illustrate simulations for a cavity QED problem [14], namely a single damped two-level system strongly coupled to a cavity mode which is driven by a broadband thermal light field [15]. We have chosen these particular examples because (i) they provide a spectrum of typical quantum-optics questions and problems, and (ii) exact solutions are available which allow an assessment of the accuracy and reliability of the simulation methods. Appendixes A–D contain technical details on the simulation of finite resolution spectra, subtraction of the coherent part of the spectrum and simulation of system correlation functions.

## II. WAVE-FUNCTION SIMULATION
## OF THE MASTER EQUATION

In this section we give a brief summary of the simulation procedure for vacuum, thermal, and squeezed reservoirs discussed in detail in our preceding paper [3]. Section II A summarizes the wave-function simulation in terms of quantum jumps for a general master equation, while Secs. II B and II C give specific results for a vacuum, thermal, and squeezed heat bath.

## A. General formalism

The master equation for a reduced system density operator $\rho(t)$ is, in its most general form [1],

$$\dot{\rho} = -i\,[H_{\text{sys}}, \rho]$$
$$+ \sum_\gamma \lambda_\gamma \left( a_\gamma \rho_\gamma a_\gamma^\dagger - \frac{1}{2} a_\gamma^\dagger a_\gamma \rho - \frac{1}{2} \rho a_\gamma^\dagger a_\gamma \right) , \quad (1)$$

with $H_{\text{sys}}$ a Hermitian operator (the system Hamiltonian divided by $\hbar$), $a_\gamma$ a set of system operators where the multidimensional index $\gamma$ identifies a *decay channel* of the system, and $\lambda_\gamma \geq 0$ . We rewrite Eq. (1) as

$$\dot{\rho} = A\rho + \sum_\gamma B_\gamma \rho \quad (2)$$

with

$$A\rho = -i \left( H_{\text{eff}} \rho - \rho H_{\text{eff}}^\dagger \right) \quad (3)$$

where

$$H_{\text{eff}} = H_{\text{sys}} - i\frac{1}{2} \sum_\gamma \lambda_\gamma a_\gamma^\dagger a_\gamma \quad (4)$$

is a non-Hermitian "effective" Hamiltonian, and

$$B_\gamma \rho = \lambda_\gamma a_\gamma \rho a_\gamma^\dagger . \quad (5)$$

The time evolution of $\rho(t)$ can be written in the form

$$\rho(t) = \sum_{n=0}^{\infty} \sum_{\gamma_1,\dots,\gamma_n} \int_{t_0}^{t} dt_n \int_{t_0}^{t_n} dt_{n-1} \dots \int_{t_0}^{t_2} dt_1 S_{t t_n} B_{\gamma_n} S_{t_n t_{n-1}} \cdots S_{t_2 t_1} B_{\gamma_1} S_{t_1 t_0} \rho(t_0) \quad (6)$$

with

$$S_{t t_0} \rho(t_0) = e^{-i H_{\text{eff}}(t-t_0)} \rho(t_0) e^{i H_{\text{eff}}^\dagger (t-t_0)} . \quad (7)$$

[In writing Eq. (7) we have assumed for simplicity that $H_{\text{sys}}$ is time independent.]

Following arguments given in Refs. [2, 3] we interpret (6) as the time evolution of a system in terms of "quantum jumps," and a nonunitary (dissipative) evolution between these jumps. The indices $n = 0, 1, 2, \dots$ and $\gamma_1, \dots, \gamma_n$ in Eq. (6) identify the contributions to the density matrix from the subensemble which has undergone exactly $n$ quantum jumps at times $t > t_n \geq \cdots \geq t_1 \geq t_0$ with a sequence of realizations $\gamma_1, \dots, \gamma_n$. Each of the quantum jumps is associated with the action of the operator $B_\gamma$ ($\sqrt{\lambda_\gamma} a_\gamma$), while the time evolution between the jumps is described by $S_{tt'}$ ($H_{\text{eff}}$). The exclusive probability density for the occurrence of exactly $n$ quantum jumps $(t_1, \gamma_1), \dots, (t_n, \gamma_n)$ during the time interval $[t_0, t)$ is

$$p_{[t_0,t)}(t_n, \gamma_n; \dots; t_1, \gamma_1)$$
$$= \text{Tr}_{\text{sys}} \left[ S_{t t_n} B_{\gamma_n} S_{t_n t_{n-1}} \dots B_{\gamma_1} S_{t_1 t_0} \rho(t_0) \right] . \quad (8)$$

Furthermore,

$$p_{[t_0,t)}(t, \gamma | t_n, \gamma_n; \dots; t_1, \gamma_1)$$
$$= \frac{\text{Tr}_{\text{sys}} \left[ B_\gamma S_{t t_n} B_{\gamma_n} S_{t_n t_{n-1}} \cdots B_{\gamma_1} S_{t_1 t_0} \rho(t_0) \right]}{\text{Tr}_{\text{sys}} \left[ B_{\gamma_n} S_{t_n t_{n-1}} \cdots B_{\gamma_1} S_{t_1 t_0} \rho(t_0) \right]} \quad (9)$$

is the conditional density that, given the sequence of quantum jumps $\gamma_1, \dots, \gamma_n$ has occurred at times $t_1$, $t_2, \dots, t_n$, respectively, the next quantum jump will be at time $t$ with realization $\gamma$.

A wave-function representation of $\rho(t)$ can be constructed by diagonalizing the initial density operator, $\rho(t_0) = \sum_\alpha p_\alpha |\alpha\rangle\langle\alpha|$ $(0 \leq p_\alpha \leq 1 \sum_\alpha p_\alpha = 1)$, and rewriting Eq. (6) as

$$\rho(t) = \sum_\alpha \sum_{n=0}^{\infty} \sum_{\gamma_1,\dots,\gamma_n} \int_{t_0}^{t} dt_n \int_{t_0}^{t_n} dt_{n-1} \dots \int_{t_0}^{t_2} dt_1 \, |\varphi(t|t_n,\gamma_n;\dots;t_1\gamma_1;\alpha)\rangle\langle\varphi(t|t_n\gamma_n;\dots;t_1\gamma_1;\alpha)|\, p_\alpha \quad (10)$$

where the $|\varphi(t|t_n, \gamma_n; \dots; \alpha)\rangle$ are a hierarchy of system wave functions that obey

$$i\frac{d}{dt} |\varphi(t|t_n, \gamma_n; \dots)\rangle = H_{\text{eff}} |\varphi(t|t_n, \gamma_n; \dots|\rangle \quad (t \geq t_n)$$
$$\quad (11)$$

with initial condition

$$|\varphi(t_0|\alpha)\rangle = |\alpha\rangle . \quad (12)$$

At the times of the quantum jumps

$$|\varphi(t_n|t_n, \gamma_n; \dots)\rangle = \sqrt{\lambda_{\gamma_n}} a_{\gamma_n} |\varphi(t_n|t_{n-1}, \gamma_{n-1}; \dots)\rangle$$
$$\quad (13)$$

and the wave function is reduced according to the action of the operator $\sqrt{\lambda_{\gamma_n}} a_{\gamma_n}$ [16].

The construction (10) suggests a wave function *simulation* of the reduced system density matrix in terms of Monte Carlo system wave functions $|\phi, t\rangle$ as follows.

(i) We choose a normalized initial system wave function $|\phi, t_0\rangle = |\alpha\rangle$ according to the probabilities $p_\alpha$, and set the counter $n$ for the number of quantum jumps equal to zero $(n = 0)$.

(ii) We propagate $|\phi, t\rangle$ according to

$$i\frac{d}{dt} |\phi, t\rangle = H_{\text{eff}} |\phi, t\rangle \quad (14)$$

and simulate the time $t$ and decay channel $\gamma$ of the *next*

*quantum jump* according to the conditional density

$$p(t, \gamma) = \| \sqrt{\lambda_\gamma} a_\gamma | \phi, t \rangle \|^2 \quad (t \geq t_n). \tag{15}$$

One possible way to determine $t$ and $\gamma$ is to proceed in two steps.

Step A: We find a decay time $t$ according to the *delay function* $p(t) = \sum_\gamma p(t, \gamma)$. This is conveniently done by drawing a random number $0 \leq r \leq 1$ from a uniform distribution and monitoring the norm of $|\phi, t\rangle$ until

$$\int_{t_n}^{t} dt' p(t') = 1 - \| |\phi, t\rangle \|^2 = r \in [0, 1] . \tag{16}$$

Step B: The decay channel $\gamma$ is determined from the conditional density $p(\gamma|t) = p(t, \gamma)/\sum_\gamma p(t, \gamma)$ for the given $t$.

Increasing $n \to n+1$ we identify $t_n \equiv t$ and $\gamma_n \equiv \gamma$ with the decay time and decay channel, respectively, and find the normalized wave function after the quantum jump according to

$$|\phi(t_n^+)\rangle = \sqrt{\lambda_{\gamma_n}} a_{\gamma_n} \frac{|\phi(t_n^-)\rangle}{\sqrt{\lambda_{\gamma_n}} \| a_{\gamma_n} |\phi(t_n)\rangle \|} \tag{17}$$

($t^\pm$ denote the times before and after the jump) and continue integrating (14) up to the next jump time, i.e., return to the beginning of (ii). Note that we normalize $|\phi, t\rangle$ after the quantum jump.

(iii) An approximation for the system density matrix is obtained by repeating these simulations in steps (i) and (ii) to obtain

$$\rho(t) = \left\langle\!\!\left\langle \frac{|\phi, t\rangle\langle\phi, t|}{\langle\phi, t|\phi, t\rangle} \right\rangle\!\!\right\rangle, \tag{18}$$

where $\langle\!\langle \ \rangle\!\rangle$ denotes an average over the different realizations of system wave functions.

The master equation (1) remains invariant under the transformation

$$\sqrt{\lambda_\gamma} a_i \to \sqrt{\lambda_\gamma} \bar{a}_\gamma = \sum_\alpha R_{\gamma\alpha} \sqrt{\lambda_\alpha} a_\alpha \tag{19}$$

with $R$ a unitary matrix. In this sense the jump operators for the quantum jumps in Eq. (17) are not unique, and there is infinitely many simulation prescriptions which lead to the same density matrix. Note that it is even possible to employ a different, unitarily equivalent set of jump operators at each quantum jump. Determination of the "next jump time" remains invariant under these transformations.

System correlation functions and spectra can be calculated by introducing weak probe fields in the system Hamiltonian $H_{\rm sys}$. This will be illustrated in the context of specific examples below.

### B. Master equation for a vacuum, thermal, and squeezed reservoir

The standard master equation for a system interacting with a broadband squeezed vacuum has the form

$$\begin{aligned}
\dot\rho_{\rm sys} = {}& -i[H_{\rm sys}, \rho] + \frac{1}{2}\gamma(N+1)(2c\rho c^\dagger - c^\dagger c\rho - \rho c^\dagger c) \\
& + \frac{1}{2}\gamma N(2c^\dagger \rho c - cc^\dagger \rho - \rho cc^\dagger) \\
& - \frac{1}{2}\gamma M(2c^\dagger \rho c^\dagger - c^\dagger c^\dagger \rho - \rho c^\dagger c^\dagger) \\
& - \frac{1}{2}\gamma M^*(2c\rho c - cc\rho - \rho cc).
\end{aligned} \tag{20}$$

Here $\gamma$ is related to the system-reservoir coupling. The parameter $N$ is the number of quanta per mode in the reservoir and $M$ with $N(N+1) \geq |M|^2$ is a measure of the squeezing. $c$ is a system lowering operator as it appears in the system-field coupling. To identify the decay channels $\gamma$ of the preceding section we must rewrite Eq. (20) in the normal form (1).

With the identifications $c_1 \equiv c$, $c_2 \equiv c^\dagger$, and by defining a field correlation matrix

$$(\gamma_{ij}) = \gamma \begin{pmatrix} N+1 & -M^* \\ -M & N \end{pmatrix}, \tag{21}$$

the damping term in Eq. (20) is

$$\Lambda\rho = \frac{1}{2}\sum_{i,j=1}^{2} \gamma_{ij} \left(2c_i\rho c_j^\dagger - c_j^\dagger c_i \rho - \rho c_j^\dagger c_i\right) . \tag{22}$$

Diagonalizing the Hermitian field correlation matrix $\gamma_{ij}$ by a unitary transformation $V_{i\gamma}$,

$$\gamma_{ij} = \sum_{\gamma=1}^{2} V_{i\gamma}\lambda_\gamma(V^\dagger)_{\gamma j} \qquad (i, j = 1, 2) \tag{23}$$

with eigenvalues $\lambda_\gamma \geq 0$, and defining

$$a_\gamma = \sqrt{\lambda_\gamma} \sum_{i=1}^{2} c_i V_{i\gamma} \qquad (\gamma = 1, 2) , \tag{24}$$

we find

$$\Lambda\rho = \sum_{\gamma=1}^{2} \left(a_\gamma\rho a_\gamma^\dagger - \frac{1}{2}a_\gamma^\dagger a_\gamma\rho - \frac{1}{2}\rho a_\gamma^\dagger a_\gamma\right) . \tag{25}$$

Explicitly, in the present case we have

$$\lambda_{1,2} = \gamma\left(N + \frac{1}{2} \pm \frac{1}{2}\sqrt{1 + 4|M|^2}\right) , \tag{26}$$

$$V = \begin{pmatrix} \cos\frac{\theta}{2} \, e^{-i\phi/2} & -\sin\frac{\theta}{2} \, e^{-i\phi/2} \\ \sin\frac{\theta}{2} \, e^{+i\phi/2} & \cos\frac{\theta}{2} \, e^{i\phi/2} \end{pmatrix},$$

with $\tan\theta = 2|M|$ and $M = -|M|e^{i\phi}$. Off-diagonal terms in $V_{i\gamma}$ are introduced by squeezing.

Special cases of the transformation (16), which gives the prescription for quantum jumps in the simulations according to Eq. (17), are as follows.

(i) Vacuum ($N = M = 0$): we find $\lambda_1 = \gamma$ so that

$$a_1 = c . \tag{27}$$

Thus spontaneous emission corresponds to downward

transitions, while in view of $\lambda_2 = 0$ there is no coupling to the second channel.

(ii) Thermal field ($N \neq 0, M = 0$): we have $\lambda_1 = \gamma(N+1)$, $\lambda_2 = \gamma N$ so that

$$a_1 = c, \quad a_2 = c^\dagger, \tag{28}$$

which corresponds to downward and upward quantum jumps induced by $c$ and $c^\dagger$, respectively.

(iii) Pure state squeezed vacuum ($N(N+1) = |M|^2$): we find $\lambda_1 = 2\gamma(N+\frac{1}{2})$, $\lambda_2 = 0$ with

$$a_1 = \left(\sqrt{N+1}\, e^{-i\phi/2}\, c + \sqrt{N}\, e^{+i\phi/2}\, c^\dagger / \sqrt{2N+1}\right), \tag{29}$$

which is a phase sensitive superposition of a down and up transition. Furthermore, we have again $\lambda_2 = 0$, so that there is no coupling to the second decay channel.

### C. Stochastic Schrödinger equation for vacuum, thermal, and squeezed input fields

The master equation (20) can be derived from the stochastic Schrödinger equation [3, 17]

$$d|\varphi,t\rangle = \left\{ -iH_{\text{sys}}dt - \frac{1}{2}\gamma[(N+1)c^\dagger c + Ncc^\dagger \right.$$
$$\left. -Mc^\dagger c^\dagger - M^*cc]dt \right.$$
$$\left. +\sqrt{\gamma}dB^\dagger(t)c - \sqrt{\gamma}dB(t)c^\dagger \right\}|\varphi,t\rangle, \tag{30}$$

where $dB$ and $dB^\dagger$ should be interpreted as Wiener noise increments with stochastic integration in the Ito sense (i.e., pointing to the future) obeying the Ito rules

$$dt^2 = dB(t)dt = dtdB(t) = dB^\dagger(t)dt = dtdB^\dagger(t) = 0,$$
$$dB^2(t) = Mdt,$$
$$dB^\dagger(t)^2 = M^*dt, \tag{31}$$
$$dB(t)dB^\dagger(t) = (N+1)dt,$$
$$dB^\dagger(t)dB(t) = Ndt.$$

The infinitesimal time-evolution operator corresponding to the Schrödinger equation (30) is

$$U(t+dt,t) = \exp\left[-iH_{\text{sys}}dt + \sqrt{\gamma}dB^\dagger(t)c - \sqrt{\gamma}dB(t)c^\dagger\right]$$
$$= 1 - iH_{\text{sys}}dt - \frac{1}{2}\gamma[(N+1)c^\dagger c + Ncc^\dagger$$
$$-Mc^\dagger c^\dagger - M^*cc]dt$$
$$+\sqrt{\gamma}dB^\dagger(t)c - \sqrt{\gamma}dB(t)c^\dagger .$$

Following the Ito rules it is straightforward to obtain an equation for the density operator $|\varphi,t\rangle\langle\varphi,t|$ which upon tracing over the field modes reduces to (20). Details of this procedure can be found in Ref. [3].

### III. TWO-LEVEL SYSTEM COUPLED TO VACUUM MODES

In this section we derive a simulation procedure for the weak field absorption spectrum and spectrum of res-

onance fluorescence of a two-level system driven by a strong pump field. Analytical expressions as well as a discussion of the various physical features of these spectra can be found, for example, in Refs. [8, 11, 12].

### A. Optical Bloch equations

We consider a two-level system in the presence of a strong classical electromagnetic field with amplitude $\mathcal{E}(t)$ and frequency $\omega$. The Schrödinger equation for the wave function $|\varphi,t\rangle$ in the product Hilbert space of the atom and the radiation field is, according to Ref. [3],

$$d|\varphi,t\rangle = -iH_{\text{eff}}|\varphi,t\rangle dt + \sqrt{\gamma}\, dB^\dagger(t)\sigma^-|\varphi,t\rangle , \tag{32}$$

with

$$H_{\text{eff}} = \left(-\Delta - \frac{1}{2}i\gamma\right)\sigma^+\sigma^- - \frac{\Omega}{2}\left(\sigma^+ + \sigma^-\right), \tag{33}$$

which is a special case of the stochastic Schrödinger equation (30) with $N = M = 0$. Here $\Omega = 2\mu|\mathcal{E}|$ is the Rabi frequency with $\mu$ the dipole moment of the atom, $\Delta$ is the detuning of the laser, and $\sigma^\pm$ are Pauli matrices. The Schrödinger equation is written in a frame rotating at the laser frequency. The noise term proportional to $dB^\dagger(t)$ corresponds to the generation of photons by spontaneous emission (see [3]). Equation (32) assumes a one-dimensional bath of radiation modes which in the present context gives results identical to a three-dimensional model.

The equation for the density matrix $\hat{\rho}(t) = |\varphi,t\rangle\langle\varphi,t|$ (in the product Hilbert space of the atom and the radiation field) is given by

$$d\hat{\rho}(t) = -i[H_{\text{eff}}\,\hat{\rho}(t) - \hat{\rho}(t)\,H_{\text{eff}}^\dagger]dt$$
$$+\sqrt{\gamma}[dB^\dagger(t)\sigma^-\hat{\rho}(t) + \hat{\rho}(t)\sigma^+dB(t)]$$
$$+\gamma dB^\dagger(t)\sigma^-\hat{\rho}(t)\sigma^+dB(t), \tag{34}$$

from which we derive, using $dB(t)dB^\dagger(t) = dt$, the optical Bloch equations

$$\frac{d\rho}{dt} = -i(H_{\text{eff}}\,\rho - \rho\,H_{\text{eff}}^\dagger) + \gamma\,\sigma^-\rho\,\sigma^+ \tag{35}$$

for the reduced atomic density matrix $\rho = \text{Tr}_B\{\hat{\rho}\}$ ($\text{Tr}_B$ is the trace over the radiation field). Comparison of Eq. (1) with Eq. (35) shows that in the present example we have a single decay channel (corresponding to spontaneous emission). The decay is accompanied by a transition of the electron from the excited atomic state to the ground level ($\sqrt{\lambda_1}a_1 = \sqrt{\gamma}\sigma^-$).

For the present case the Monte Carlo procedure of Sec. II A agrees with the formalism discussed in detail in one of our previous papers [2] where the simulation results are compared with the exact solution of the optical Bloch equations for the two-level system. Our simulations are based on determining the next emission time from the delay function $p(t)$. In Fig. 1 we show a comparison of a histogram distribution of decay times in a typical simulation run and the analytical result for $p(t)$ (solid line) for $\Delta = 0$ and $\Omega = 3\gamma$. The time evolution of $p(t)$ shows
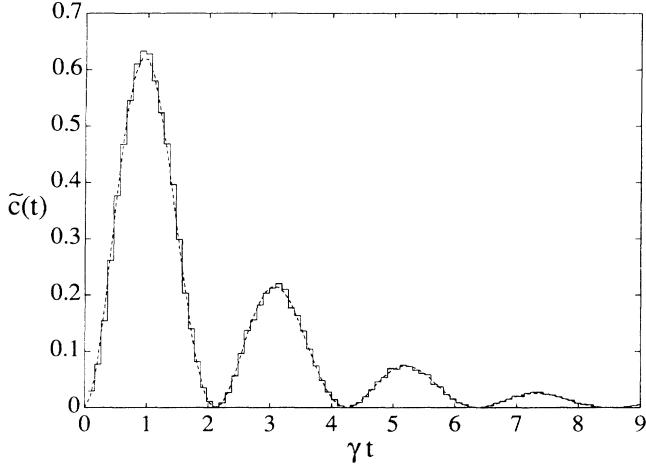
FIG. 1. Comparison of a histogram distribution of decay times in a typical simulation run and the analytical result for the delay function $p(t)$ (solid line) for $\Delta = 0$ and $\Omega = 3\gamma$.

damped Rabi oscillations. Furthermore, as part of our simulations we obtain information on the photon statistics of the emitted light. In Fig. 2 we plot as an example the simulation results and the analytical expressions (solid line) for the Mandel $Q$ parameter as a function of detuning $\Delta$ ($\Omega = \gamma$). The Mandel parameter is defined as

$$\frac{\langle n^2 \rangle - \langle n \rangle^2}{\langle n \rangle} = 1 + Q, \tag{36}$$

with $n$ the number of emitted photons. $Q$ is a measure of the deviation from Poisson statistics, with $Q < 0$ and $Q > 0$ corresponding to sub-top and super-Poissonian statistics, respectively [10].

## B. Absorption spectrum

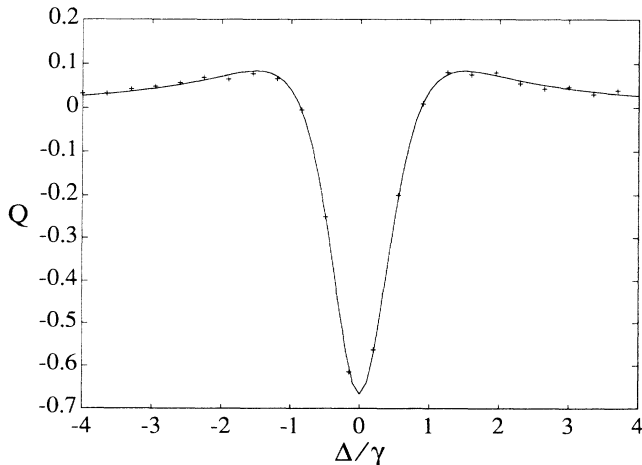We now apply a small probe field to the two-level system. The corresponding effective Hamiltonian is



FIG. 2. Mandel $Q$ parameter as a function of detuning for $\Omega = \gamma$; crosses indicate simulation results, solid lines correspond to the analytical solution for $Q$.

$$\tilde{H}_{\text{eff}}(t) = H_{\text{eff}} - \frac{\delta\Omega}{2}\left(\sigma^+\,e^{-i(\nu t + \eta)} + \sigma^-\,e^{+i(\nu t + \eta)}\right), \tag{37}$$

where $\delta\Omega = 2\mu|\delta\mathcal{E}|$ and $\eta$ are the Rabi frequency and phase of the probe field, respectively; $\nu$ is the detuning between the probe and pump field frequencies. With the ansatz

$$|\varphi, t\rangle = |\varphi_0, t\rangle + \frac{\delta\Omega}{2}\left(e^{-i(\nu t + \eta)}|\beta_+^\nu, t\rangle\right.$$
$$\left. + e^{+i(\nu t + \eta)}\,|\beta_-^\nu, t\rangle\right) + O\left(\delta\Omega^2\right) \tag{38}$$

we derive from Eq. (32) for $|\varphi, t\rangle$ the equations

$$d|\varphi_0, t\rangle = -iH_{\text{eff}}\,|\varphi_0, t\rangle dt + \sqrt{\gamma}\,dB^\dagger(t)\sigma^-|\varphi_0, t\rangle, \tag{39}$$

$$d|\beta_\pm^\nu, t\rangle = -i(H_{\text{eff}} \mp \nu)|\beta_\pm^\nu, t\rangle dt + \sqrt{\gamma}\,dB^\dagger(t)\sigma^-|\beta_\pm^\nu, t\rangle$$
$$+ i\sigma^\pm|\varphi_0, t\rangle dt.$$

An analogous expansion for the total atom plus field density matrix $\hat{\rho}(t) = |\varphi, t\rangle\langle\varphi, t|$ is

$$\hat{\rho}(t) = \hat{\rho}_0(t) + \frac{\delta\Omega}{2}[\,\hat{\rho}_+(t)\,e^{-i(\nu t + \eta)}$$
$$+ \hat{\rho}_-(t)\,e^{+i(\nu t + \eta)}\,] + O\left(\delta\Omega^2\right), \tag{40}$$

with

$$\hat{\rho}_0(t) = |\varphi_0, t\rangle\langle\varphi_0 t|,$$
$$\hat{\rho}_\pm(t) = |\beta_\pm^\nu, t\rangle\langle\varphi_0, t| + |\varphi_0, t\rangle\langle\beta_\mp^\nu, t|. \tag{41}$$

This leads to the following equation for the first-order perturbed density matrices $\hat{\rho}_\pm$:

$$d\hat{\rho}_\pm = -i\left(H_{\text{eff}}\hat{\rho}_\pm - \hat{\rho}_\pm H_{\text{eff}}^\dagger \mp \nu\hat{\rho}_\pm\right)dt$$
$$+ \sqrt{\gamma}\,[dB^\dagger(t)\sigma^-\,\hat{\rho}_\pm + \hat{\rho}_\pm\,\sigma^+ dB(t)]$$
$$+ \gamma dB^\dagger(t)\sigma^-\,\hat{\rho}_\pm\,\sigma^+\,dB(t) + i\left[\sigma^\pm, \hat{\rho}_0\right]dt, \tag{42}$$

while the equation for the zeroth-order term $\hat{\rho}_0$ is identical to Eq. (34). By tracing over the radiation field and using $dB(t)dB^\dagger(t) = dt$, we obtain

$$\dot{\rho}_0 = -i\left(H_{\text{eff}}\,\rho_0 - \rho_0\,H_{\text{eff}}^\dagger\right) + \gamma\sigma^-\,\rho_0\,\sigma^+, \tag{43}$$

$$\dot{\rho}_\pm = -i\left(H_{\text{eff}}\,\rho_\pm - \rho_\pm\,H_{\text{eff}}^\dagger \mp \nu\rho_\pm\right)$$
$$+ \gamma\,\sigma^-\,\rho_\pm\,\sigma^+ + i\left[\sigma^\pm, \rho_0\right].$$

The rate of absorption from the probe beam is given by ([8, 11])

$$W(\nu) = \frac{-i\delta\Omega^2}{4}\,Tr_A\left\{\sigma^+\,\rho_-(t)\right\} + \text{c.c.} \quad (t \to \infty), \tag{44}$$

or in terms of $|\beta_\pm^\nu, t\rangle$ and $|\varphi_0, t\rangle$

$$W(\nu) = \frac{-i\delta\Omega^2}{4} \left( \langle\varphi_0, t|\sigma^+|\beta^\nu_-, t\rangle + \langle\beta^\nu_+, t|\sigma^+|\varphi_0, t\rangle \right)$$

$$+\text{c.c.} \quad (t \to \infty), \qquad (45)$$

where the first and second terms correspond to induced emission and absorption, respectively. In deriving (44) and (45) we have averaged over the phase $\eta$ of the probe laser [11]. For completness we mention that the above expression for $W(\nu)$ can be rewritten in the form

$$W(\nu) = \frac{\delta\Omega^2}{4} \int_0^t dt' \, e^{-i\nu(t-t')} \, \langle [\sigma^+(t), \sigma^-(t')] \rangle + \text{c.c.}$$

$$(t \to \infty), \qquad (46)$$

which is the Fourier transform of the two-time correlation function for $\sigma^\pm(t)$. Equation (46) follows from Eq. (44) with the help of the quantum fluctuation regression theorem. Analytical expressions for $W(\nu)$ can be found in Ref. [11].

From the above considerations we derive the following simulation:

$$|\phi, t\rangle = |\phi_0, t\rangle + \frac{\delta\Omega}{2} \left( |B^\nu_+, t\rangle \, e^{-i(\nu t + \eta)} \right.$$

$$\left. + |B^\nu_-, t\rangle \, e^{+i(\nu t + \eta)} \right); \qquad (47)$$

we get for the zeroth- and first-order contributions

$$\frac{d|\phi_0, t\rangle}{dt} = -iH_\text{eff}|\phi_0, t\rangle, \qquad (48)$$

$$\frac{d|B^\nu_\pm, t\rangle}{dt} = -i\left(H_\text{eff} \mp \nu\right)|B^\nu_\pm, t\rangle + i\sigma^\pm \, |\phi_0, t\rangle. \qquad (49)$$

The absorption spectrum is given in terms of these Monte Carlo wave functions by

$$W(\nu)$$

$$= \frac{-i\delta\Omega^2}{4} \left\langle\!\!\left\langle \frac{\left( \langle\phi_0, t|\sigma^+|B^\nu_-, t\rangle + \langle B^\nu_+, t|\sigma^+|\phi_0, t\rangle \right)}{\||\phi_0, t\rangle\|^2} \right\rangle\!\!\right\rangle$$

$$+\text{c.c.} \quad (t \to \infty). \qquad (50)$$

The absorption spectrum $W(\nu)$ , Eq. (50), is accurate to second order in the probe field; it is therefore sufficient to determine the jump times in the simulations to zeroth order in the probe field from Eq. (48) for $|\phi_0, t\rangle$. Furthermore, the simulation wave functions in Eq. (50) must be normalized with respect to $|\phi, t\rangle$; in view of $\||\phi_0, t\rangle\|^2 = \||\phi_0, t\rangle\|^2 + O(\delta\Omega)$ it is sufficient to normalize with respect to the zeroth-order wave function $|\phi_0, t\rangle$. The condition for the quantum jumps

$$|\phi, t^+\rangle = \sigma^- \, |\phi, t^-\rangle / \|\sigma^- \, |\phi, t^-\rangle\| \qquad (51)$$

leads to the jump conditions in each order

$$|\phi_0, t^+\rangle = \sigma^- \, |\phi_0, t^-\rangle / \|\sigma^- \, |\phi_0, t^-\rangle\|,$$

$$\qquad (52)$$

$$|B^\nu_\pm, t^+\rangle = \sigma^- \, |B^\nu_\pm, t^-\rangle / \|\sigma^- \, |\phi_0, t^-\rangle\|.$$

To summarize, the absorption spectrum can be simulated by propagating the set of first-order equations for $|B^\nu_\pm, t\rangle$ driven by the zeroth-order wave function $|\phi_0, t\rangle$, which dictates the quantum jump.

Figures 3(a) and 3(b) show a comparison of analytical and numerical simulation results of the absorption spectrum $W(\nu)$ for various parameters. Analytical results [11] are represented by solid lines, while simulations are plotted as crosses. The parameters are $\Omega = 4 \, \gamma$, $\Delta = 0$ [Fig. 3(a)], and $\Delta = \gamma$ [Fig. 3(b)]. Positive values of $W(\nu)$ indicate absorption, while regions with $W < 0$ correspond to gain. We have simulated a finite-resolution spectrum by adding a small bandwidth $\epsilon = \frac{\gamma}{10}$ to the probe laser. We thereby avoid problems due to the coherent contribution to the emission and absorption parts of the spectrum (a $\delta$ function at $\nu = 0$ which cancels in the total absorption spectrum). As shown in Appendix A, finite resolution amounts to substituting $\pm\nu \to \pm\nu - i\epsilon$ in Eqs. (49) provided the absorption spectrum is calculated according to Eq. (45). Explicit subtraction of the coherent components of spectra is discussed in Appendix B. The simulation results of Fig. 3 were obtained by propagating the zeroth-order wave function $|\phi_0, t\rangle$ to the stationary (long-time) limit and integrating the set of equations for $|B^\nu_\pm, t\rangle$ for a vector of frequencies $\nu$ in parallel. Instead of an ensemble average, we have computed a time average of a single realization.

We made an error analysis to determine the rate of convergence of our simulation procedure for the absorption spectrum. We determined for fixed $\Omega, \Delta$, and $\gamma$ the standard deviation $\sigma$ (scaled to the maximum of $W$ as a function of $\nu$) according to

$$\sigma = \frac{\max\limits_{\nu} \sqrt{\sum\limits_{i=1}^{M}[W_i^{(N)}(\nu) - W(\nu)]^2/M}}{\max\limits_{\nu} |W(\nu)|} \approx \frac{\alpha}{\sqrt{N}}$$
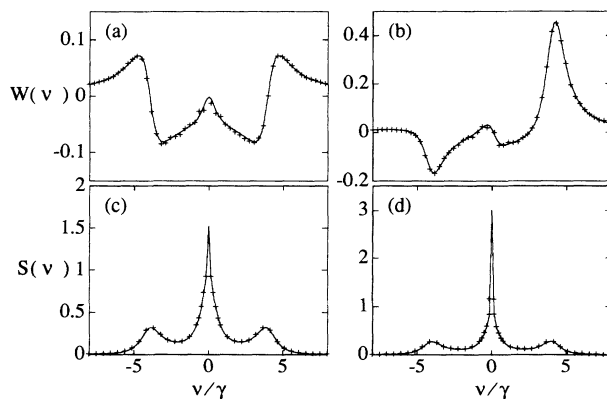
$$(M \to \infty) \quad (53)$$



FIG. 3. Absorption (a) and (b) and fluorescence (c) and (d) spectra as a function of $\nu/\gamma$ for $\Omega = 4 \, \gamma$ and $\Delta=0$ and $\gamma$, respectively. The solid lines are analytical results, while the crosses correspond to our simulations for $10^4$ (a) and (c) and $10^5$ samples (b) and (d). $W(\nu)$ is plotted in units of $\delta\Omega^2/\gamma$. The resolution bandwidth is $\epsilon = \frac{1}{10}\gamma$. The fluorescence spectrum contains both the coherent and incoherent part.

with $W_i^{(N)}$ the $i$th simulation value for a given number of realizations $N$. For $\Delta = \gamma$ and $\Omega = \gamma, 2\gamma, 4\gamma$ we found $\alpha \approx 0.36, 0.45, 0.74$, while for $\Delta = 0$ and $\Omega = \gamma, 2\gamma, 4\gamma$, we obtained $\alpha \approx 0.75, 1.05, 1.89$. Thus to achieve an accuracy of roughly 1%, roughly $10^4$ realizations were necessary. Figures 3(a) and 3(b) were calculated using $10^5$ and $10^4$ realizations, respectively.

The formalism of the present section is based on probing the atom with a monochromatic probe field. A spectrum is obtained by simulating a set of first-order wave functions corresponding to a vector of frequencies $\nu$. Alternatively, we can probe the system by a white-noise probe field to provide us with system time-correlation functions. In this method only a single first-order equation (and not a set of equations) has to be integrated at the expense of simulating a white-noise driving field in addition to quantum jumps (for details see Appendix C). A method of simulating system correlation functions based on "kicking" the system with $\delta$-function pulses is outline in Appendix D. A simulation procedure for atomic correlation functions has also been given by Dalibard, Castin, and Mølmer [4].

### C. The resonance fluorescence spectrum

We treat the fluorescence spectrum separately, although this simply corresponds to the emission part of the absorption spectrum computed using the algorithm described above. The spectrum of resonance fluorescence of a two-level system is given by (see Ref. [3])

$$S(\nu) = \frac{1}{t} \langle \varphi, t | r^\dagger(\nu, t) r(\nu, t) | \varphi, t \rangle \quad (t \to \infty), \quad (54)$$

with the operator $r(\nu, t)$ given by

$$r(\nu, t) = \int_0^t e^{-i\nu(t-s)} dB(s). \quad (55)$$

Thus the calculation of the spectrum amounts to determining the norm of the vector $|\beta^\nu, t\rangle = r(\nu, t)|\varphi, t\rangle$, i.e., $S(\nu) = \frac{1}{t} \langle \beta^\nu, t | \beta^\nu, t \rangle$ $(t \to \infty)$. In the stationary limit this is identical to

$$S(\nu) = \frac{d}{dt} \left( \langle \beta^\nu, t | \beta^\nu, t \rangle \right) \quad (t \to \infty). \quad (56)$$

The equation for $|\beta^\nu, t\rangle$ is

$$d|\beta^\nu, t\rangle = -i(H_{\text{eff}} + \nu)|\beta^\nu, t\rangle dt + \sqrt{\gamma} dB^\dagger(t) \sigma^- |\beta^\nu, t\rangle$$
$$+ \sqrt{\gamma} \sigma^- |\varphi, t\rangle dt, \quad (57)$$

(where we used $dB(t)|\varphi, t\rangle = 0$). Thus

$$S(\nu) = -i\sqrt{\gamma} \left( \langle \varphi, t | \sigma^+ | \beta^\nu, t \rangle + \text{c.c.} \right) \quad (t \to \infty). \quad (58)$$

The equation for $|\beta^\nu, t\rangle$ is, apart from a different factor in the inhomogeneous term, identical to the equation for $|\beta^\nu_-, t\rangle$ [see Eq. (39)], and the spectrum of resonance fluorescence is, apart from an overall factor, identical to the emission term in expression (45) for the absorption spectrum. Note that the spectrum is the Fourier transform of the atomic two-time correlation function

$$S(\nu) = \gamma \int_0^t e^{-i\nu(t-t')} dt' \, \langle \sigma^+(t)\sigma^-(t') \rangle + \text{c.c.} \quad (59)$$

The formalism outlined above is a stochastic Schrödinger equation version of the Mollow's treatment of the spectrum of resonance fluorescence [8].

The resulting simulation algorithm is analogous to the one derived in Sec. III B (the fluorescence spectrum is just the emission part of the absorption spectrum). We propagate the system wave function $|\phi, t\rangle$ and the first-order wave function $|B^\nu, t\rangle$ according to

$$\frac{d|\phi, t\rangle}{dt} = -iH_{\text{eff}}|\phi, t\rangle,$$

$$\frac{d|B^\nu, t\rangle}{dt} = -i\left(H_{\text{eff}} + \nu\right)|B^\nu, t\rangle + i\sqrt{\gamma}\sigma^-|\phi, t\rangle. \quad (60)$$

The random decay time is determined from the norm of $|\phi, t\rangle$, and the condition for the quantum jump is

$$|\phi, t^+\rangle = \sigma^- |\phi, t^-\rangle / \|\sigma^-|\phi, t^-\rangle\|,$$

$$|B^\nu, t^+\rangle = \sigma^- |B^\nu, t^-\rangle / \|\sigma^-|\phi, t^-\rangle\|. \quad (61)$$

Again, $|B^\nu, t\rangle$ is propagated in parallel with $|\phi, t\rangle$ by solving the above equation with the $|\phi, t\rangle$-dependent inhomogenity. The spectrum is given by averaging over these realizations

$$S(\nu) = -i\sqrt{\gamma} \left\langle\!\!\left\langle \frac{\langle \phi, t | \sigma^+ | B^\nu, t \rangle}{\||\phi, t\rangle\|^2} + \text{c.c.} \right\rangle\!\!\right\rangle \quad (t \to \infty). \quad (62)$$

In Figs. 3(c) and 3(d) we show a comparison of our simulations (crosses) with analytical results [8] (solid lines) for the Mollow spectrum [12]. The parameters are the same as for the absorption spectrum. These spectra contain the coherent part which has been smoothed out due to our assumption of a finite resolution detector with width $\epsilon = \frac{\gamma}{10}$ (see Appendix A). An explicit subtraction of the coherent part is discussed in Appendix B. Again we find that to get the same accuracy we need more realizations in the on-resonance case than in the off-resonance case (we chose $10^4$ realizations for the off-resonance case, while on-resonance we chose $10^5$) (see error analysis in Sec. III B).

### IV. TWO-LEVEL ATOM COUPLED TO A SQUEEZED VACUUM

In recent years a body of work has been produced on the interaction of squeezed light with atoms, following largely from the initial work of Gardiner [13] in which it was shown that squeezed light may inhibit the decay of one of the polarization quadratures of the atom and thus give rise to a subnatural linewidth in the fluorescence spectrum.

The non-Hermitian effective Hamiltonian and the jump operator required for a Monte Carlo simulation of the master equation for a system interacting with a

squeezed vacuum have already been detailed in Sec. II. For a two-level atom interacting with a squeezed vacuum we have

$$H_{\text{eff}} = -\Delta\sigma^+\sigma^- - \frac{1}{2}i\gamma(N+1)\sigma^+\sigma^- - \frac{1}{2}i\gamma N\sigma^-\sigma^+,$$

(63)

and for the jump operator

$$a_1 = (\sqrt{N+1}e^{-i\phi/2}\sigma^- + \sqrt{N}e^{i\phi/2}\sigma^+)/\sqrt{2N+1},$$

(64)

where we have transformed to the rotating frame, and $\Delta$ is the detuning between the atomic transition frequency and the carrier frequency of the squeezed field. As noted in Sec. II B, this jump operator is a phase-sensitive superposition of raising and lowering operators, and hence a quantum jump will in general project the atom into a phase-sensitive superposition of ground and excited states. This has very interesting consequences if one considers a single trajectory of the Bloch vector, as described by the three components $\langle\sigma_x\rangle = \langle\sigma^+ + \sigma^-\rangle$, $\langle\sigma_y\rangle = -i\langle(\sigma^+ - \sigma^-)\rangle$, and $\langle\sigma_z\rangle = \langle\sigma^+\sigma^- - \sigma^-\sigma^+\rangle$. Such a trajectory is shown in Fig. 4. The phase has been chosen so that the $\langle\sigma_x\rangle$ component is aligned with the reduced-noise quadrature of the squeezed field, while $\langle\sigma_y\rangle$
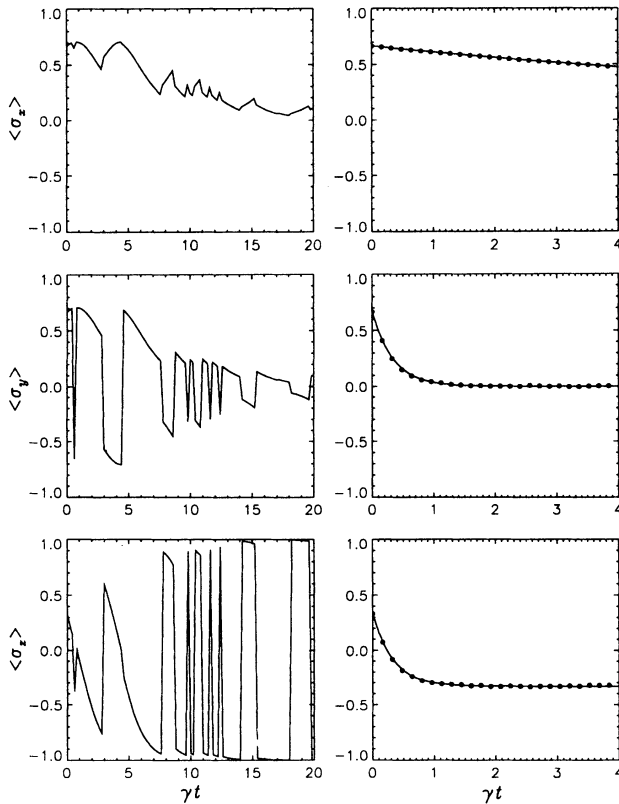


FIG. 4. Time evolution of the Bloch vector components for a two-level atom in a squeezed vacuum, with $N = 1$, $\phi = 0$, and $\Delta = 0$: (a) single trajectory, (b) average of 10 000 trajectories (solid circles) with theoretical results (solid lines).

is aligned with the increased-noise quadrature. One observes that the behavior of $\langle\sigma_x\rangle$ with each quantum jump is very different from that of $\langle\sigma_y\rangle$ and $\langle\sigma_z\rangle$. In contrast to the relatively small interruptions experienced by $\langle\sigma_x\rangle$, $\langle\sigma_y\rangle$, and $\langle\sigma_z\rangle$ reverse sign with each quantum jump, and ultimately $\langle\sigma_z\rangle$ behaves simply as it would with a thermal field, jumping between $-1$ and $+1$ as the atom absorbs and emits photons. The difference in the behavior of the Bloch vector components with each quantum jump leads to a dramatic difference in the averaged behavior of the components, as shown also in Fig. 4 where the average of 10 000 trajectories has been taken. The decay rate of $\langle\sigma_x\rangle$ is significantly slower than in an ordinary vacuum, while that of $\langle\sigma_y\rangle$ and $\langle\sigma_z\rangle$ is significantly enhanced. In these plots the simulation is compared with theory and again the agreement is very good.

In the fluorescence spectrum, the inhibition of the decay of $\langle\sigma_x\rangle$ results in a subnatural linewidth. Again, our simulation procedure for computing spectra is able to reproduce all of the analytical results, including those which incorporate a coherent driving field in addition to the squeezed field [18].

## V. TWO-LEVEL ATOM STRONGLY COUPLED TO A CAVITY DRIVEN BY A THERMAL FIELD

The system consisting of a single two-level atom strongly coupled to a high-finesse cavity is presently of considerable theoretical and experimental interest. Multiple exchanges of photons between the atom and the quantized cavity mode can yield interesting quantum dynamical processes. Notable predictions for this system include steady-state atomic population inversion [19], squeezing and antibunching [20], and optical bistability [21]. In recent (optical) experiments, vacuum Rabi splitting has been observed [14].

From a theoretical point of view, this configuration in the strong-coupling regime represents a somewhat challenging problem. The relative magnitude and importance of quantum fluctuations at the single-atom level means that semiclassical approaches, based, for example, on the derivation of a Fokker-Planck equation from the quantum master equation, can no longer be applied. In addition, the problem of high dimensionality arises since the description of the cavity mode entails use of the infinite Fock state basis. Truncation at a modest level can still lead to an extremely large problem if one attempts to solve the master equation directly.

The Monte Carlo simulation procedure described in this paper is well suited to this problem since (i) it operates at the quantum level, without semiclassical approximations, and (ii) it deals with wave functions, thereby reducing the dimensionality considerably from that associated with a density-matrix approach. In this section, we will describe our simulation procedure for the atom-cavity configuration, concentrating on parameter regimes of some relevance to current experiments.

We will consider a cavity mode driven by a broadband thermal light field. Recent theoretical work by Cirac, Ritsch, and Zoller [15] has yielded analytical results for

quantities of interest with which we can compare our simulations. Our model is easily generalized to include a coherent driving field, but for the purposes of describing our procedure a thermal field suffices. We note that some work on wave function simulations of the coupled atom-cavity system with a coherent driving field has been presented by Carmichael [5].

## A. Simulation procedure

The Ito stochastic Schrödinger equation for a two-level atom coupled to a cavity mode (annihilation operator $a$) driven by broadband thermal light can be written as

$$d|\varphi, t\rangle = -iH_{\text{eff}}|\varphi, t\rangle + \sqrt{\gamma}\, dB^\dagger(t)\sigma^-|\varphi, t\rangle$$
$$+ \sqrt{2\kappa}\, dG^\dagger(t)a|\varphi, t\rangle + \sqrt{2\kappa}\, dG(t)a^\dagger|\varphi, t\rangle ,\quad (65)$$

where

$$H_{\text{eff}} = -\frac{\Delta}{2}\sigma^+\sigma^- + ig(a^\dagger\sigma^- - a\sigma^+)$$
$$- i\kappa(N+1)a^\dagger a - i\kappa Naa^\dagger - i\frac{\gamma}{2}\sigma^+\sigma^- ,\quad (66)$$

and $dB(t)$ and $dG(t)$ represent the vacuum modes into which the atom decays and the thermal field entering the cavity, respectively. That is, $dB(t)$ and $dG(t)$ are independent Wiener processes satisfying

$$dBdB^\dagger = dt , \quad dB^\dagger dB = dB^2 = dB^{\dagger 2} = 0 ,$$
$$(67)$$
$$dGdG^\dagger = (N+1)dt , \quad dG^\dagger dG = Ndt , \quad dG^2 = dG^{\dagger 2} = 0,$$

with $N$ the mean photon number of the thermal field. In the above, $\Delta = \omega_c - \omega_a$ is the detuning of the cavity mode from the atomic transition frequency, $g$ is the atom-field coupling constant, $\gamma$ is the spontaneous emission rate of the atom into modes outside the cavity, and $\kappa$ is the decay rate of the cavity field. Using Ito calculus, the corresponding master equation for this system can be derived in the familiar form

$$\frac{d\rho}{dt} = i\frac{\Delta}{2}[\sigma_z, \rho] + g[a^\dagger\sigma^- - a\sigma^+, \rho]$$
$$+ \frac{\gamma}{2}\left(2\sigma^-\rho\sigma^+ - \sigma^+\sigma^-\rho - \rho\sigma^+\sigma^-\right)$$
$$+ \kappa(N+1)(2a\rho a^\dagger - a^\dagger a\rho - \rho a^\dagger a)$$
$$+ \kappa N(2a^\dagger\rho a - aa^\dagger\rho - \rho aa^\dagger) .\quad (68)$$

Rewriting this master equation in the form (2) we identify the three possible decay channels as

$$B_1\rho = \gamma\sigma^-\rho\sigma^+,$$
$$B_2\rho = 2\kappa(N+1)a\rho a^\dagger,\quad (69)$$
$$B_3\rho = 2\kappa Na^\dagger\rho a,$$

with corresponding jump operators

$$\sqrt{\lambda_1}a_1 = \sqrt{\gamma}\sigma^- ,$$
$$\sqrt{\lambda_2}a_2 = \sqrt{2\kappa(N+1)}a,\quad (70)$$
$$\sqrt{\lambda_3}a_3 = \sqrt{2\kappa N}a^\dagger.$$

The jump operator $a_1$ corresponds to the emission of a fluorescence photon out the sides of the cavity. The operators $a_2$ and $a_3$ correspond, respectively, to the loss of a photon through the cavity mirrors and to the absorption of a photon from the thermal light field.

The basis set for this system is of course infinite, so for practical purposes we must introduce a truncated basis set, the size of which will be determined by the degree of excitation (i.e., by the intensity of the driving field) in the system. We truncate the Fock basis set at a particular number state $|s\rangle$, and define the cavity annihilation operator to be

$$a = \sum_{n=1}^{s} \sqrt{n}|n-1\rangle\langle n| .\quad (71)$$

States of the system are denoted by $|g\rangle|n\rangle \equiv |g, n\rangle$ and $|e\rangle|n\rangle \equiv |e, n\rangle$ where $|e\rangle$ and $|g\rangle$ are the excited and ground states of the two-level atom, respectively, and we represent the wave function for the system in the form

$$|\phi, t\rangle = c_0^g(t)|g, 0\rangle + \sum_{n=0}^{s-1}\left\{c_n^e(t)|e, n\rangle + c_{n+1}^g(t)|g, n+1\rangle\right\} .$$
$$(72)$$

This particular representation is chosen because in solving the equation $i\partial_t|\phi, t\rangle = H_{\text{eff}}|\phi, t\rangle$ with $H_{\text{eff}}$ given by (66), one derives a set of equations for $c_n^{g,e}(t)$ in which $c_n^e(t)$ couples only to $c_{n+1}^g(t)$. This coupling, together with the possible quantum jumps between the states, is depicted schematically in Fig. 5. We note that the addition of a coherent driving field complicates this picture somewhat, but the representation for $|\phi, t\rangle$ is easily generalized to this situation.

Our procedure for simulating the master equation for the atom-cavity system follows that described in the previous section. Using $i\partial_t|\phi, t\rangle = H_{\text{eff}}|\phi, t\rangle$, we propagate the wave function $|\phi, t\rangle$ from some initial time $t_0$ (at which $\langle\phi, t_0|\phi, t_0\rangle = 1$) until the time $t_D$ at which the norm of $|\phi, t\rangle$ has decayed to the value of the random number $r \in (0,1)$ chosen from a uniform distribution. Having determined the time at which the transition takes place, we must then decide which of the three possible jumps actually occurs. To do this, we use a second uniformly distributed random number to choose between the three jumps to which we assign the conditional densities

$$p(t, 1) = \|a_1|\phi, t\rangle\|^2 = \gamma\sum_{n=0}^{s-1}|c_n^e(t)|^2,$$

$$p(t, 2) = \|a_2|\phi, t\rangle\|^2$$
$$= 2\kappa(N+1)\left\{\sum_{n=1}^{s-1}n|c_n^e(t)|^2\right.$$
$$\left. + \sum_{n=0}^{s-1}(n+1)|c_{n+1}^g(t)|^2\right\},\quad (73)$$

$$p(t, 3) = \|a_3|\phi, t\rangle\|^2$$
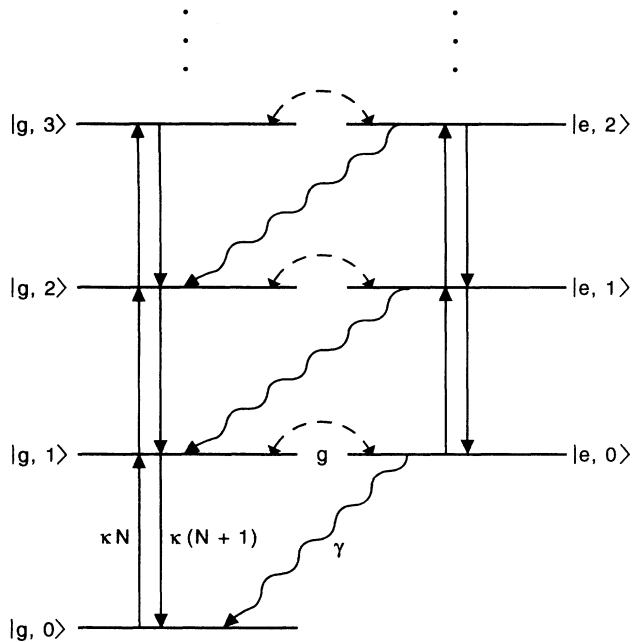$$= 2\kappa N\left\{\sum_{n=0}^{s-2}(n+1)|c_n^e(t)|^2 + \sum_{n=0}^{s-1}(n+1)|c_n^g(t)|^2\right\}.$$

FIG. 5. Schematic of the coupled atom-cavity system showing possible transitions between basis states.

Once the nature of the jump has been established, the new (normalized) wave function is formed using (17). The entire procedure is repeated many times to construct a single trajectory, and a solution for the density matrix is generated by averaging over many such trajectories.

## B. Numerical results

### 1. Atomic inversion and cavity photon number

For the purpose of illustrating the simulation procedure in this multilevel quantum system, it is worthwhile following a single trajectory of the cavity photon number $\langle a^\dagger a \rangle$ and the atomic inversion $\langle \sigma_z \rangle$, as we have done in Fig. 6. The system is initially in its ground state $|g, 0\rangle$ before the absorption of a photon from the thermal field raises it to the first excited state $|g, 1\rangle$. An oscillatory exchange of excitation between the cavity mode and the atom (i.e., an oscillation of the population between the pair of states $|g, 1\rangle$ and $|e, 0\rangle$) then follows, until the absorption of a second thermal photon raises the system to the next pair of excited states $\{|g, 2\rangle, |e, 1\rangle\}$. After a short time in these states, two successive one-photon emissions return the system to the ground state at $\gamma t \simeq 1.2$. Another such sequence of excitations and emissions commences at $\gamma t \simeq 2.5$. In this second sequence, we note the difference between the oscillation frequencies (which vary approximately as $g\sqrt{n+1}$) corresponding to different pairs of states $\{|g, n+1\rangle, |e, n\rangle\}$. In Fig. 6 we have also shown the time development of the norm of the wave function ($\langle \phi | \phi \rangle$) for this particular trajectory. This serves to illustrate how the decay rate of the norm depends upon which states are currently populated. The higher the ex-

cited state, the faster the decay of the norm.

The time development of the averages of quantities such as the cavity photon number and the atomic inversion are computed by averaging over many such trajectories. For steady-state averages we can follow a single trajectory, taking samples at intervals such that consecutive samples are independent of each other. The results of such a procedure are given in Fig. 7, where we plot the steady-state values of $\langle a^\dagger a \rangle / N$ and $\langle \sigma_z \rangle$ as a function of the coupling parameter $g$. The simulation results were obtained from averages of 10 000 samples, and the basis set was truncated at $s = 10$ (i.e., a total of 21 basis states). The solid lines in Fig. 7 are the analytical results computed using the approach of Cirac, Ritsch, and Zoller [15]. The agreement between the two approaches is generally at the level of a few percent or better with this number of samples. We have estimated the standard deviation in our results for several data points and have plotted error bars accordingly. This standard deviation decreases with further sampling and would appear to exhibit a linear dependence on the inverse square root of the number of samples.
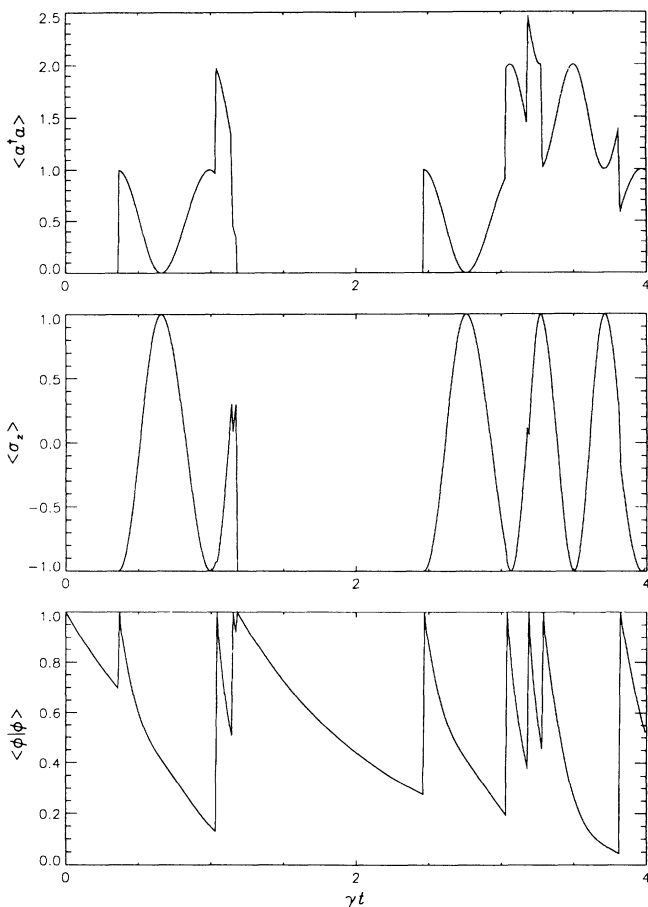


FIG. 6. Single trajectory of the cavity photon number $\langle a^\dagger a \rangle$, atomic inversion $\langle \sigma_z \rangle$, and the norm $\langle \phi | \phi \rangle$, for $N = 1$, $g = 5\gamma$, and $\kappa = 0.25\gamma$.
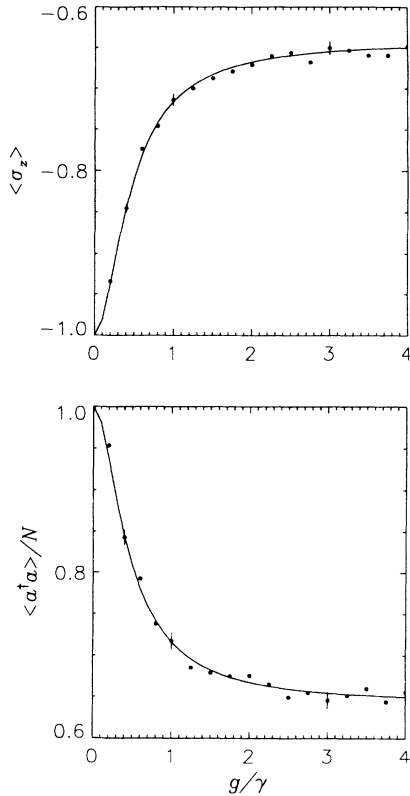
FIG. 7.  Steady-state cavity photon number and atomic inversion as a function of the coupling parameter $g/\gamma$ for $N = 0.5$, $\kappa = 0.5\gamma$. The simulation results are computed from 10 000 samples and solid line is computed from the theory of Cirac, Ritsch, and Zoller [15].
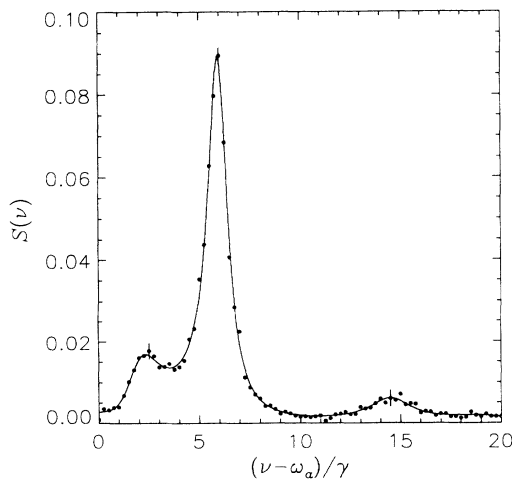


FIG. 8.  Fluorescence spectrum emitted by the atom out the sides of the cavity for $N = 1$, $\kappa = 0.1\gamma$, $g = 6\gamma$. The simulation results are computed from 50 000 samples and the solid line is computed from the theory of Cirac, Ritsch, and Zoller [15].

### 2. Fluorescence spectrum

The methods described in Secs. III B and III C for the computation of spectra are straightforwardly modified to the coupled atom-cavity system. As an example, we have computed by simulation the spectrum of resonance fluorescence emitted by the atom out the sides of the cavity,

$$S(\nu) = \lim_{t \to \infty} \text{Re} \int_0^\infty d\tau \, e^{-i\nu\tau} \langle \sigma^+(t + \tau)\sigma^-(t)\rangle. \quad (74)$$

Our results are shown in Fig. 8, again compared with the theory of Cirac, Ritsch, and Zoller. Error bars at several points again represent estimates of the standard deviation of our results for this particular number of samples. The peak that one associates with the vacuum Rabi splitting is the dominant feature at the frequency $\nu = \omega + g$. For this particular parameter set, one also sees additional sidebands. These are discussed in detail by Cirac, Ritsch, and Zoller, and correspond to transitions between different dressed states of the coupled system.

## VI. CONCLUSIONS

In this paper we have considered a variety of examples from quantum optics to demonstrate the application and implementation of wave-function simulation techniques to solve the quantum master equation. The examples considered include (i) the calculation of the absorption and emission spectrum of a two-level system coupled to vacuum modes of the radiation field, (ii) the dynamics of a two-level system interacting with a broadband squeezed vacuum, and (iii) a strongly coupled atom-cavity system with the atom coupled to a reservoir of vacuum modes and the cavity driven by a broadband thermal field. The choice of these particular examples was motivated by the availability of exact solutions which allowed us to evaluate and confirm the success and applicability of the simulation method in the context of quantum optics. We have generalized and adapted the simulation procedures of the present paper to the solution of the quantum master equation of complex quantum optical systems, such as calculation of atomic spectra for laser cooling in the quantum limit (for multilevel atoms in one-dimensional configurations [22,23]), and cavity QED problems involving coherent driving fields and coupling to a squeezed vacuum.

*Note added.* We have recently received a copy of unpublished work from K. Mølmer, Y. Castin, and J. Dalibard which also describes applications of the Monte Carlo wave-function approach to problems in quantum optics, but with emphasis on mechanical light effects.

## APPENDIX A: SIMULATION
## OF FINITE-RESOLUTION SPECTRA

In this appendix we generalize the simulation procedure of Sec. III for the absorption spectrum $W(\nu)$ and spectrum of resonance fluorescence $S(\nu)$ to compute *finite-resolution spectra*, i.e., spectra which are averaged over a finite resolution bandwidth $\epsilon$. In part, we were motivated to do this in order to circumvent numerical problems arising from the coherent part of the spectrum ($\delta$-function components corresponding to elastic scattering). Explicit subtraction of the coherent part of the spectrum is discussed in Appendix B.

*Absorption spectrum of a two-level system.* We assume a probe laser with finite bandwidth $\epsilon$. In particular the phase $\eta(t)$ in Eq. (37) is taken to obey the phase diffusion equation $d\eta(t) = \sqrt{2\epsilon}dW(t)$ where $W(t)$ is a Wiener process [1]. This corresponds to a Lorentzian probe laser spectrum with full width at half maximum $2\epsilon$. For the stochastically averaged absorption rate (45) we find

$$W = \frac{-i\delta\Omega^2}{4}\langle\!\langle(\langle\varphi_0,t|\sigma^+|\beta_-^\nu,t\rangle$$
$$+\langle\beta_+^\nu,t|\sigma^+|\varphi_0,t\rangle)\rangle\!\rangle_{\text{PD}}+\text{c.c.}, \qquad \text{(A1)}$$

where $\langle\!\langle\ \rangle\!\rangle_{\text{PD}}$ indicates averaging over the phase diffusion noise. As only the $|\beta_\pm^\nu,t\rangle$ depend on the probe phase $\eta$, the averaging in (A1) can be pulled through $\langle\varphi_0,t|$ and $\sigma^+$. Thus we need to consider only the stochastically averaged evolution equations for $\langle\!\langle\ |\beta_\pm^\nu,t\rangle\rangle\!\rangle_{\text{PD}}$. A stochastic phase $\eta(t)$ leads to a fluctuating frequency $[\nu+\dot\eta(t)]$ in Eq. (39). The resulting equation has to be interpreted in the Stratonovich sense [1]. It is easily converted, however, to the Ito form

$$d|\beta_\pm^\nu,t\rangle = -i(H_{\text{eff}}\mp\nu-i\epsilon)\,|\beta_\pm^\nu,t\rangle dt$$
$$+\sqrt{\gamma}\,dB^\dagger(t)\sigma^-|\beta_\pm^\nu,t\rangle$$
$$\pm i\sqrt{2\epsilon}\,dW(t)|\beta_\pm^\nu,t\rangle+i\sigma^\pm|\varphi_0,t\rangle. \qquad \text{(A2)}$$

Averaging gives

$$d\langle\!\langle\ |\beta_\pm^\nu,t\rangle\rangle\!\rangle_{\text{PD}} = -i(H_{\text{eff}}\mp\nu-i\epsilon)\,\langle\!\langle\ |\beta_\pm^\nu,t\rangle\rangle\!\rangle_{\text{PD}}dt$$
$$+\sqrt{\gamma}\,dB^\dagger(t)\sigma^-\langle\!\langle\ |\beta_\pm^\nu,t\rangle\rangle\!\rangle_{\text{PD}}$$
$$+i\sigma^\pm|\varphi_0,t\rangle\ , \qquad \text{(A3)}$$

where we have used $\langle dW(t)\cdots\rangle_{\text{PD}} = 0$. Thus we see that averaging over the probe laser spectrum amounts to the substitution

$$\pm\nu\rightarrow\pm\nu-i\epsilon. \qquad \text{(A4)}$$

For the simulation functions $|B_\pm,t\rangle$ (47) analogous arguments can be made with the result that a finite-resolution spectrum can be simulated by making the

substitution (A4) in Eq. (48) provided the absorption spectrum is calculated from (50) (which is linear in $\langle\!\langle\ |B_\pm^\nu,t\rangle\rangle\!\rangle_{\text{PD}}$).

*Resonance fluorescence.* For the Mollow spectrum we assume a radiation detector with finite-resolution described by a Lorentzian filter function

$$D(\nu) = \frac{\epsilon}{\pi}\ \frac{1}{\nu^2+\epsilon^2}. \qquad \text{(A5)}$$

The spectrum that one actually measures is $S_\epsilon(\nu) = S(\nu-i\epsilon)$. Again going back to the evolution equations for the system wave functions $|B,t\rangle$ we use the stochastically averaged equations for $|B,t\rangle$ which amounts to the replacement $+i\nu\rightarrow i\nu-\epsilon$. Again we emphasize that this is valid only because the spectrum (50) is linear in $|B^\nu,t\rangle$.

## APPENDIX B: SUBTRACTION
## OF THE COHERENT PART
## OF THE FLUORESCENCE SPECTRUM

As shown in Sec. III, the spectrum is related to the two-time correlation function for the atomic operators [Eq. (59)]. The coherent part (which leads to the $\delta$ function in the spectrum) is given by

$$S_{\text{coh}}(\nu) = \int_0^t e^{-i\nu(t-t')}\ \langle\sigma^+(t)\rangle\langle\sigma^-(t')\rangle+\text{c.c.}\quad(t\rightarrow\infty).$$
$$\text{(B1)}$$

In terms of the wave function simulation

$$S_{\text{coh}}(\nu) = \left\langle\!\!\left\langle\int_0^t e^{-i\nu(t-t')}\ \langle\sigma^-(t')\rangle\langle\phi_0,t|\sigma^+|\phi_0,t\rangle dt'\right\rangle\!\!\right\rangle$$
$$(t\rightarrow\infty). \quad \text{(B2)}$$

We define

$$|\tilde B,t\rangle = |B,t\rangle - \int_0^t e^{-i\nu(t-t')}\ \langle\sigma^-(t')\rangle dt'|\phi_0,t\rangle, \qquad \text{(B3)}$$

so the incoherent part of the spectrum is given by

$$S(\nu) - S_{\text{coh}}(\nu) = \langle\!\langle\langle\phi_0,t|\sigma^+|\tilde B,t\rangle\rangle\!\rangle + \text{c.c.} \qquad \text{(B4)}$$

$|\tilde B,t\rangle$ obeys the equation

$$i\frac{d}{dt}|\tilde B,t\rangle = (H_{\text{eff}}+\nu)\,|\tilde B,t\rangle+i\sqrt{\gamma}\left[\sigma^- - \langle\sigma^-(t)\rangle\right]|\phi_0,t\rangle,$$
$$\text{(B5)}$$

where the value of $\langle\sigma^-(t)\rangle(t\rightarrow\infty)$ must be taken from a previous simulation of the stationary values of $\rho$. So subtraction of the coherent part amounts to replacing $\sigma^\pm$ by $\sigma^\pm - \langle\sigma^\pm\rangle$. This is consistent with the relation

$$S_{\text{inc}}(\nu) + S_{\text{coh}}(\nu) = \int_0^t e^{-i\nu(t-t')}\ \langle\ [\sigma^+(t') - \langle\sigma^+(t')\rangle]\ [\sigma^-(t) - \langle\sigma^-(t)\rangle]\ \rangle$$
$$+\int_0^t e^{-i\nu(t-t')}\ \langle\sigma^+(t)\rangle\langle\sigma^-(t')\rangle + \text{c.c.} = S(\nu)\ (t\rightarrow\infty). \qquad \text{(B6)}$$

Thus the coherent part of the spectrum is subtracted by simulating Eq. (B5) with a modified source term corresponding to a subtraction of the mean value of the dipole operator in the driving term.

## APPENDIX C: CALCULATING TWO-TIME ATOMIC CORRELATION FUNCTIONS BY PROBING WITH WHITE NOISE

The purpose of this appendix is to give an outline of a formalism to calculate system two-time correlation functions by probing a system with white noise. To be specific, we restrict our discussion to a two-level system.

*Absorption spectrum.* In Sec. III we have calculated the atomic absorption and emission spectrum by probing the atom with a (weak) monochromatic field of frequency $\nu$. These spectra are Fourier transforms of stationary two-time atomic correlations functions [see Eqs. (46) and (59)]. Here we probe the atom with a (complex) white-noise field and obtain the atomic two-time correlation functions directly by cross correlating the time-delayed white noise with the first-order response of the atom. To first order we write

$$\rho(t) = \rho_0(t) + \frac{\delta\Omega}{2}\rho_1(t) + O(\delta\Omega^2) \tag{C1}$$

($\delta\Omega$ is a measure of the strength of the probe field). $\rho_0(t)$ is the density matrix of the two-level system in the presence of the pump field only, and $\rho_1(t)$ is the first-order correction due to the probe field, obeying the equation of motion,

$$\dot{\rho}_0(t) = \mathcal{L}_0\rho_0(t), \tag{C2}$$

$$\dot{\rho}_1(t) = \mathcal{L}_0\rho_1(t) + \mathcal{L}_1(t)\rho_0(t). \tag{C3}$$

The first of these equations is the optical Bloch equation (35), and

$$\mathcal{L}_1(t)\rho = i[\sigma^-\eta(t) + \sigma^+\eta^*(t), \rho] . \tag{C4}$$

This corresponds to adding a time-dependent Hamiltonian $-\frac{1}{2}\delta\Omega[\eta(t)\sigma^- + \text{H.c.}]$ to the Hamiltonian (33), where $\eta(t)$ is a complex white noise with

$$\langle \eta^*(t)\eta(t')\rangle_{\text{WN}} = \delta(t - t'),$$
$$\langle \eta(t)\eta(t')\rangle_{\text{WN}} = 0, \tag{C5}$$
$$\langle \eta(t)\rangle_{\text{WN}} = 0.$$

The first-order reponse of the atom is

$$\rho_1(t) = \int_0^t dt' e^{\mathcal{L}_0(t-t')}\mathcal{L}_1(t')\rho_0(t'), \tag{C6}$$

which gives for $\tau > 0$

$$\lim_{t\to\infty} \left\langle\!\!\left\langle -i\,\eta^*(t-\tau)\text{Tr}_A\left\{\sigma^+\rho_1(t)\right\}\right\rangle\!\!\right\rangle_{\text{WN}} \tag{C7}$$

$$= \text{Tr}_A\left\{\sigma^+ e^{\mathcal{L}_0\tau}\left[\sigma^-, \rho_s\right]\right\} = \langle[\sigma^+(\tau), \sigma^-(0)]\rangle, \quad \text{(C8)}$$

where we have used the quantum fluctuation regression theorem ($\rho_s$ is the stationary solution for the density matrix of the atom). According to Eq. (46) this correlation function gives the absorption spectrum.

From the stochastic wave function $|\varphi, t\rangle$, we get by means of the ansatz

$$|\varphi, t\rangle = |\varphi_0, t\rangle + \frac{\delta\Omega}{2}|\beta, t\rangle \tag{C9}$$

the equations

$$d|\varphi_0, t\rangle = -iH_{\text{eff}}|\varphi_0, t\rangle dt + \sqrt{\gamma}\,dB^\dagger(t)\sigma^-|\varphi_0, t\rangle, \tag{C10}$$

$$d|\beta, t\rangle = -iH_{\text{eff}}|\beta, t\rangle dt + \sqrt{\gamma}\,dB^\dagger(t)\sigma^-|\beta, t\rangle$$
$$+ i[\eta(t)\sigma^- + \text{H.c.}]|\varphi_0, t\rangle dt . \tag{C10}$$

These equations could have been derived immediately from Eq. (39) by defining

$$|\beta, t\rangle = \sum_\nu e^{-i\nu t}\eta_\nu|\beta^\nu_+, t\rangle + e^{i\nu t}\eta^*_\nu|\beta^\nu_-, t\rangle, \tag{C11}$$

$$\eta(t) = \sum_\nu \eta_\nu e^{-i\nu t}$$

(with $\eta_\nu$ complex coefficients). The two-time correlation function of Eq. (C7) is given by

$$\langle[\sigma^+(\tau), \sigma^-(0)]\rangle = -i \left\langle\!\!\left\langle \eta^*(t-\tau)\left(\langle\beta, t|\sigma^+|\varphi_0, t\rangle + \langle\varphi_0, t|\sigma^+|\beta, t\rangle\right)\right\rangle\!\!\right\rangle_{\text{WN}} \quad (t \to \infty, \tau > 0). \tag{C12}$$

The corresponding simulation procedure of the Monte Carlo wave function follows by expanding the Monte Carlo system wave function $|\phi, t\rangle = |\phi_0, t\rangle + \frac{\delta\Omega}{2}|B, t\rangle$, which gives

$$\frac{d}{dt}|\phi_0, t\rangle = -iH_{\text{eff}}|\phi_0, t\rangle, \tag{C13}$$

$$\frac{d}{dt}|B, t\rangle = -iH_{\text{eff}}|B, t\rangle + i[\eta(t)\sigma^- + \eta^*(t)\sigma^+]|\phi_0, t\rangle. \tag{C14}$$

The conditions for quantum jumps follow from Eq. (51). In simulating Eq. (C13) two stochastic elements: quantum jumps (quantum noise) and a (classical) additive noise term which can be integrated by standard techniques [1]. The two-time correlation functions are

$$\langle[\sigma^+(\tau), \sigma^-(0)]\rangle - i\left\langle\!\!\left\langle \left\langle\!\!\left\langle \frac{\langle B, t|\eta^*(t-\tau)\sigma^+|\phi_0, t\rangle + \langle\phi_0, t|\eta^*(t-\tau)\sigma^+|B, t\rangle}{\|\phi_0, t\rangle\|^2}\right\rangle\!\!\right\rangle_{\text{WN}}\right\rangle\!\!\right\rangle \quad (t \to \infty, \tau > 0). \tag{C15}$$

*Resonance fluorescence.* The correlation functions relevant for calculating the resonance fluorescence spectrum could be obtained from Eq. (57) by an expansion similar to Eq. (C11)

$$|\beta, t\rangle = \sum_{\nu} e^{+i\nu t} \eta_{\nu} |\beta_+^{\nu}, t\rangle, \tag{C16}$$

$$\eta(t) = \sum_{\nu} \eta_{\nu} e^{i\nu t} + \text{c.c.} \tag{C17}$$

(where it is sufficient to take $\eta_{\nu}$ as real coefficients). The resulting equations are

$$d|\varphi_0, t\rangle = -iH_{\text{eff}} |\varphi_0, t\rangle dt + \sqrt{\gamma} \, dB^{\dagger}(t)\sigma^- |\varphi_0, t\rangle, \tag{C18}$$

$$\begin{aligned} d|\beta, t\rangle = &-iH_{\text{eff}}|\beta, t\rangle dt + \sqrt{\gamma} \, dB^{\dagger}(t)\sigma^- |\beta, t\rangle \\ &+ i\eta(t)\sigma^- |\varphi_0, t\rangle dt. \end{aligned}$$

Accordinq to Eqs. (58) and (59),

$$-i\langle \varphi_0, t|\sigma^+|\beta, t\rangle = \int_0^t \eta(t') \, \langle \sigma^+(t)\sigma^-(t')\rangle. \tag{C19}$$

Therefore the two-time correlation functions are given by

$$-i\langle\!\langle \, \eta(t-\tau)\langle\varphi_0, t|\sigma^+|\beta, t\rangle \rangle\!\rangle_{\text{WN}} = \langle \sigma^+(\tau)\sigma^-(0)\rangle$$
$$(t \to \infty, \tau > 0). \tag{C20}$$

The resulting simulation procedure is analogous to that described for the absorption spectrum.

## APPENDIX D: TWO-TIME ATOMIC CORRELATION FUNCTIONS BY PROBING WITH $\delta$ KICKS

In this appendix we show that system correlation functions can be calculated by probing the system with short pulses (assumed to be $\delta$ functions). System spectra can then be found from the Fourier transfrom of these correlation functions. To be specific we restrict our discussion again to the absorption and emission spectrum of a two-level system [see Eqs. (46) and (59)].

*Absorption spectrum.* We add time dependent Hamiltonian $-\frac{1}{2}\delta\Omega[\delta(t-t_0)(\sigma^- + \sigma^+)]$ to the Hamiltonian (33) ($t_0$ is the time when the kick occurs), and write to first order

$$\rho(t) = \rho_0(t) + \frac{\delta\Omega}{2}[\rho_+(t) + \rho_-(t)] + O(\delta\Omega^2) \tag{D1}$$

($\delta\Omega$ is the strength of the delta kick). Here $\rho_0(t)$ is the stationary density matrix of the two-level system in the presence of the pump field, and $\rho_{\pm}(t)$ are the first-order corrections. The equation for $\rho_0(t)$ is the optical Bloch equation (35), in shorthand $\dot{\rho}_0(t) = \mathcal{L}_0\rho_0(t)$, while the equations for $\rho_{\pm}(t)$ have the form

$$\dot{\rho}_{\pm}(t) = \mathcal{L}_0\rho_1(t) + \mathcal{L}_{\pm}(t)\rho_0(t), \tag{D2}$$

with

$$\mathcal{L}_{\pm}(t)\rho = i\delta(t - t_0)[\sigma^{\pm}, \rho]. \tag{D3}$$

Thus the first-order response of the atom is for times $t > t_0$

$$\rho_{\pm}(t) = ie^{\mathcal{L}_0(t-t_0)}[\sigma^{\pm}, \rho_0(t_0)], \tag{D4}$$

which gives for the stationary correlation function

$$\lim_{t\to\infty} i \, \text{Tr}_A \left\{ \sigma^{\mp}\rho_{\pm}(t) \right\} = \langle [\sigma^{\pm}(t), \sigma^{\mp}(t_0)]\rangle. \tag{D5}$$

In the deriving this equation we used the quantum fluctuation regression theorem.

The same arguments can be repeated on the level of the wave functions. From the stochastic wave function $|\varphi, t\rangle$, we get by means of the ansatz

$$|\varphi, t\rangle = |\varphi_0, t\rangle + \frac{\delta\Omega}{2}(|\beta_-, t\rangle + |\beta_+, t\rangle) \tag{D6}$$

the equations

$$d|\varphi_0, t\rangle = -iH_{\text{eff}} |\varphi_0, t\rangle dt + \sqrt{\gamma} \, dB^{\dagger}(t)\sigma^- |\varphi_0, t\rangle, \tag{D7}$$

$$\begin{aligned} d|\beta_{\pm}, t\rangle = &-iH_{\text{eff}}|\beta_{\pm}, t\rangle dt + \sqrt{\gamma} \, dB^{\dagger}(t)\sigma^- |\beta_{\pm}, t\rangle \\ &+ i\delta(t - t_0)\sigma^{\pm} |\varphi_0, t\rangle dt. \end{aligned}$$

The two-time correlation functions are given by

$$\begin{aligned} \langle [\sigma^+(t), \sigma^-(t_0)]\rangle = &-i(\langle\varphi_0, t|\sigma^+|\beta_-, t\rangle \\ &+ \langle\beta_+, t|\sigma^+|\varphi_0, t\rangle) \end{aligned}$$
$$(t \to \infty, t > t_0). \tag{D8}$$

The simulation procedure for the Monte Carlo wave function follows by expanding $|\phi, t\rangle = |\phi_0, t\rangle + \frac{\delta\Omega}{2}(|B_+, t\rangle + |B_-, t\rangle)$, which gives

$$\frac{d}{dt}|\phi_0, t\rangle = -iH_{\text{eff}}|\phi_0, t\rangle,$$
$$\frac{d}{dt}|B_{\pm}, t\rangle = -iH_{\text{eff}}|B_{\pm}, t\rangle + i\delta(t - t_0)\sigma^{\pm}|\phi_0, t\rangle. \tag{D9}$$

Due to the $\delta$ function in the inhomogenity the equations for the $|B_{\pm}, t\rangle$ are easily integrated with the result that the $|B_{\pm}, t\rangle$ obey the same homogeneous equation as $|\phi_0, t\rangle$ but with initial condition

$$|B_{\pm}, t = t_0\rangle = i\sigma_{\pm}|\phi_0, t_0\rangle. \tag{D10}$$

The quantum jumps follow from Eq. (51). The simulation approximation for two-time correlation functions is

$$\langle [\sigma^+(t), \sigma^-(t_0)]\rangle$$
$$= -i\left\langle\!\!\left\langle \frac{\langle\phi_0, t|\sigma^+|B_-, t\rangle + \langle B_+, t|\sigma^+|\phi_0, t\rangle}{\||\phi_0, t\rangle\|^2} \right\rangle\!\!\right\rangle$$
$$(t \to \infty, t > t_0). \tag{D11}$$

In this equation averaging over randomly distributed $t_0$ is implied so that the correlation function becomes stationary in time, i.e., is a function of $t - t_0$.

*Resonance fluorescence.* The above arguments can be repeated to calculated and simulate the correlation functions for resonance fluorescence. The relevant correlation function corresponds to the first term in Eq. (D11)

$$\langle \sigma^+(t)\sigma^-(t_0) \rangle = -i \left\langle\!\!\left\langle \frac{\langle \phi_0, t | \sigma^+ | B_-, t \rangle}{\| |\phi_0, t\rangle \|^2} \right\rangle\!\!\right\rangle$$

$$(t \to \infty, t > t_0). \quad \text{(D12)}$$

[1] C. W. Gardiner, *Quantum Noise* (Springer-Verlag, Berlin, 1992); *Handbook of Stochastic Methods* (Springer-Verlag, Berlin, 1985).

[2] R. Dum, P. Zoller, and H. Ritsch, Phys. Rev. A **45**, 4879 (1992).

[3] C. W. Gardiner, A. S. Parkins, and P. Zoller, preceding paper, Phys. Rev. A **46**, 4363 (1992).

[4] J. Dalibard, Y. Castin, and K. Mølmer, Phys. Rev. Lett. **68**, 580 (1992).

[5] H. J. Carmichael (unpublished).

[6] C. Cohen-Tannoudji, F. Bardou, and A. Aspect, in *Laser Spectroscopy X*, edited by M. Ducloy, E. Giacobino, and G. Camy (World Scientific, Singapore, 1992).

[7] R. Blatt and P. Zoller, Eur. J. Phys. **9**, 250 (1988); C. Cohen-Tannoudji and J. Dalibard, Europhys. Lett. **1**, 441 (1986); G. C. Hegerfeldt, in *Proceedings of the International Wigner Symposium at Golsar* (World Scientific, Singapore, 1992); H. J. Carmichael, S. Singh, R. Vyas, and P. R. Rice, Phys. Rev. A **39**, 1200 (1989); R. J. Cook, Prog. Opt. **28**, 361 (1990).

[8] B. R. Mollow, Phys. Rev. A **12**, 1919 (1975).

[9] M. D.Srinivas and E. B. Davies, Opt. Acta **28**, 981 (1981).

[10] L. Mandel, Opt. Lett. **4**, 205 (1979).

[11] B. R. Mollow, Phys. Rev. A **5**, 2217 (1972).

[12] B. R. Mollow, Phys. Rev. **188**, 1969 (1969).

[13] C. W. Gardiner, Phys. Rev. Lett. **56**, 1917 (1986).

[14] M. G. Raizen, R. J. Thompson, R. J. Brecha, H. J. Kimble, and H. J. Carmichael, Phys. Rev. Lett. **63**, 240 (1989).

[15] J. I. Cirac, H. Ritsch, and P. Zoller, Phys. Rev. A **44**, 4541 (1991).

[16] Equations (10)–(13) represent a generalization of Mollow's wave-function representation of optical Bloch equations as given in Ref. [8].

[17] A. Barchielli, Phys. Rev. A **34**, 1642 (1986); J. Phys. A **20**, 6341 (1987).

[18] H. J. Carmichael, A. S. Lane, and D. F. Walls, Phys. Rev. Lett. **58**, 2539 (1987).

[19] C. M. Savage, Phys. Rev. Lett. **60**, 1829 (1988).

[20] H. J. Carmichael, Phys. Rev. Lett. **55**, 2790 (1985).

[21] C. M. Savage and H. J. Carmichael, IEEE J. Quantum Electron. **24**, 1495 (1988).

[22] D. Grison, B. Louis, C. Salomon, J. Y. Courtois, and G. Grynberg, Europhys. Lett. **15**, 149 (1991).

[23] J. W. R. Tabosa, G. Chen, Z. Hu, R. B. Lee, and H. J. Kimble, Phys. Rev. Lett. **66**, 3245 (1991).